Journal of Marine Science and Technology

Volume 28 | Issue 6 Article 5

Dynamic Modelling and Experimental Results of a Ray-Type Hybrid Underwater Glider with a Dualbuoyancy Engine

Ngoc-Duc Nguyen
Department of Electrical and Information Engineering, Seoul National University of Science and Technology, Seoul, South Korea

Hyeung-Sik Choi
Department of Mechanical Engineering, Korea Maritime and Ocean University, Busan, South Korea, hchoi@kmou.ac.kr

Sung-Wook Lee
Department of Naval Architecture and Ocean System Engineering, Korea Maritime and Ocean University, Busan, South Korea

Wen-Hsiang Hsieh
Department of Automation, National Formosa University, Taiwan.

Sang-Ki Jeong
Maritime ICT R&D Center, Korea Institute of Ocean Science & Technology, Busan, Korea

See next page for additional authors

Recommended Citation

Nguyen, Ngoc-Duc; Choi, Hyeung-Sik; Lee, Sung-Wook; Hsieh, Wen-Hsiang; Jeong, Sang-Ki; and Ji, Dae-Hyeong (2020) "Dynamic Modelling and Experimental Results of a Ray-Type Hybrid Underwater Glider with a Dualbuoyancy Engine," *Journal of Marine Science and Technology*: Vol. 28: Iss. 6, Article 5.
DOI: DOI:10.6119/JMST.202012_28(6).0005
Available at: https://jmstt.ntou.edu.tw/journal/vol28/iss6/5

Dynamic Modelling and Experimental Results of a Ray-Type Hybrid Underwater Glider with a Dualbuoyancy Engine

Acknowledgements

This is results of the research project entitled “data collecton system with underwater glider” (19-SN-MU-01) and is a part of the result of the research project (18-SN-RB-01).

Authors

Ngoc-Duc Nguyen, Hyeung-Sik Choi, Sung-Wook Lee, Wen-Hsiang Hsieh, Sang-Ki Jeong, and Dae-Hyeong Ji

Journal of Marine Science and Technology, Vol. 28, No. 6, pp. 502-506 (2020)
DOI: 10.6119/JMST.202012_28(6).0005

DYNAMIC MODELLING AND EXPERIMENTAL RESULTS OF A RAY-TYPE HYBRID UNDERWATER GLIDER WITH A DUALBUOYANCY ENGINE

Ngoc-Duc Nguyen[1], Hyeung-Sik Choi[2], Sung-Wook Lee[3] , Wen-Hsiang Hsieh[4], Sang-Ki Jeong[5], and Dae-Hyeong Ji[6]

Key words: underwater glider; dual-buoyancy engine; dynamic modelling.

ABSTRACT

For ocean observation and exploration, underwater gliders (UG) have shown their efficient long-range operation with buoyancy propulsion. The current Torpedo-shape UGs have small buoyancy capacity and insufficient space for batteries and sensors. In this paper, a Ray-type hybrid underwater glider (RHUG) is developed with new hull design, dual-buoyancy engine, and thrusters. The control system of the RHUG is constructed for gliding motion. To understand the characteristic of the RHUG, dynamic modelling of the dual-buoyancy engine was established. To verify the proposed dynamics model, a navigation experiment using the developed RHUG platform was carried out. Through comparison between experiment and simulation results, the validity of dynamic modelling will be presented. And the experimental results in the sea are also illustrated to evaluate the gliding performance of this new hull design.

I. INTRODUCTION

Since ocean data is essential for predicting typhoons and climate changes, the usage of underwater glider (UG) is one of the most effective way to collect real-time ocean data. The very first design of UG is presented and showed their efficiency in long-range operation (Webb et al., 2001; Sherman et al., 2001). A 3000m class of underwater glider was designed for mooring application and its motion was only simulated (Nakamura et al., 2013). A variable buoyancy profiler was developed with the same concept of underwater glider using model predictive control to generate the depth plan (Smith and Huynh, 2013) and only simulation was conducted in this research. The steady-state input for a miniature glider was provided from the steady-state gliding motion (Zhang et al., 2013), and the gliding performance was analyzed depending on movable mass displacement and net buoyancy input. The lift-drag ratio of blended-wing UG was increased using the flying wing design (Wang et al., 2015), then the simulation of this design showed better gliding efficiency. The stabilizer and rudder were designed for blended-wing-body underwater glider and their stability and maneuverability were simulated (Ma et al., 2018). Smartfloat was developed (Cao et al., 2019) with the capability of floater and underwater glider, and several sea trials were conducted to show promising results.

In this study, a new hull design of hybrid underwater glider is proposed. The capacity of buoyancy engine is increased by using dual buoyancy engine inside the ray-shaped hull. Hydrodynamic coefficients of gliding dynamics are presented in non-dimensional form. And then, the mathematical model of RHUG is studied and verified through simulations and experiments. Finally, some successful gliding results of RHUG is presented.

II. VEHICLE MODELLING

1. Vehicle description

The shape of Ray-type hybrid underwater glider looks like the flat fish with the specification in Table 1. The hull of the

Paper submitted 04/16/19; revised 05/06/20; accepted 07/08/20. Corresponding Author: Hyeung-Sik Choi (e-mail: hchoi@kmou.ac.kr)
[1] Department of Electrical and Information Engineering, Seoul National University of Science and Technology, Seoul, South Korea
[2] Department of Mechanical Engineering, Korea Maritime and Ocean University, Busan, South Korea.
[3] Department of Naval Architecture and Ocean System Engineering, Korea Maritime and Ocean University, Busan, South Korea.
[4] Department of Automation, National Formosa University, Taiwan.
[5] Maritime ICT R&D Center, Korea Institute of Ocean Science & Technology, Busan, Korea.
[6] Marine Security and Safety Research Center, Korea Institute of Ocean Science & Technology, Busan, South Korea.

Table 1. RHUG parameters

Parameters	Value
L×W×H	1.67×1.22×0.18m
Static mass	70kg
Position of static mass	[−0.0061;0;0]m
Moving mass	1.5kg
Position of movable mass	0.193m<x_m<0.373m
Inertia of static mass	*diag*([1.28;2.89;4.17])kgm^2
Net buoyancy	±0.7kg
Position of left buoyancy engine	[0.34;0.112;0]m
Position of right buoyancy engine	[0.34;−0.112;0]m

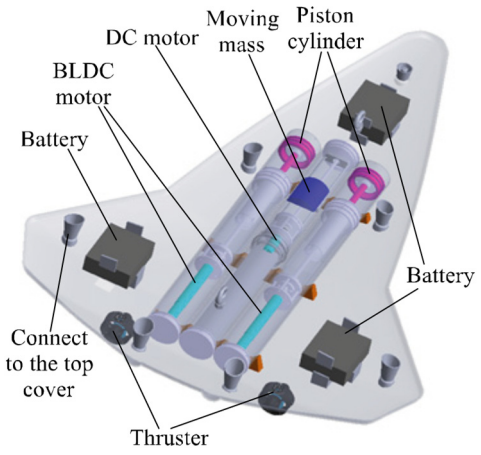

Fig. 1. Design of RHUG

RHUG is designed as one bottom and one top cover which are connected by bolts and nuts at 8 connecting points showed in Figure 1. There are two buoyancy engine blocks, one mass-shifter block and 3 places of batteries. The piston-cylinder is the key mechanism of buoyancy engine. The middle block contains the hardware of control system and the moving mass. Two buoyancy blocks are connected with the control system by SubComn cables. And the test bed is manufactured as shown in Figure 2.

2. Dynamics of 6-DOF

The six-degrees of freedom model of a fully submerged underwater vehicle can be described as:

$$\begin{aligned}
&m\left[\dot{u}-vr+wq-x_g\left(q^2+r^2\right)+y_g\left(pq-\dot{r}\right)+z_g\left(pr+\dot{q}\right)\right]=X\\
&m\left[\dot{v}-wp+ur-y_g\left(r^2+p^2\right)+z_g\left(qr-\dot{p}\right)+x_g\left(qp+\dot{r}\right)\right]=Y\\
&m\left[\dot{w}-wq+vp-z_g\left(p^2+q^2\right)+x_g\left(rp-\dot{q}\right)+y_g\left(rq+\dot{p}\right)\right]=Z\\
&I_x\dot{p}+\left(I_z-I_y\right)qr+m[y_g\left(\dot{w}-uq+vp\right)-z_g(\dot{v}-wp+ur)]=K\\
&I_y\dot{q}+\left(I_x-I_z\right)rp+m[z_g\left(\dot{u}-vr+wq\right)-x_g(\dot{w}-uq+vp)]=M\\
&I_z\dot{r}+\left(I_y-I_x\right)pq+m\left[x_g\left(\dot{v}-wp+ur\right)-y_g\left(\dot{u}-vr+wq\right)\right]=N
\end{aligned} \tag{1}$$

Table 2. Dimensionless hydrodynamics coefficients (CFD method).

Parameters	Value	Parameters	Value
$X_{\dot{u}}$	–0.003013	$Z_{\dot{w}}$	–0.011836
X_{uu}	–0.001812	$Z_{\dot{q}}$	–0.004774
X_{qq}	–0.00292	Z_{uu}	0.019815
X_{ww}	0.02244	Z_q	–0.087055
X_{wq}	–0.043862	Z_w	–0.484655
$M_{\dot{w}}$	–0.022352	$Z_{w\|w\|}$	–0.584865
$M_{\dot{q}}$	–0.003823	M_{uu}	0.002994
M_q	–0.04598	$M_{q\|q\|}$	–0.19927
M_w	0.024439	$M_{w\|w\|}$	–0.213197

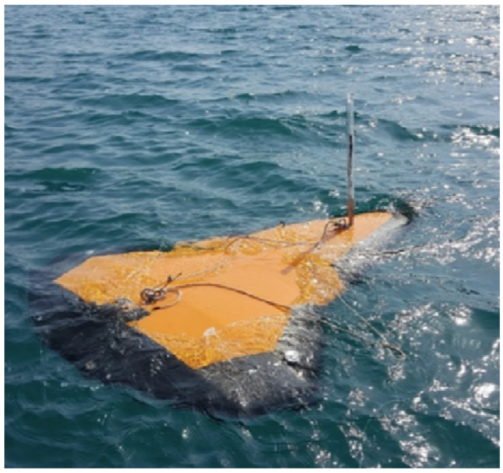

Fig. 2. RHUG in the sea test

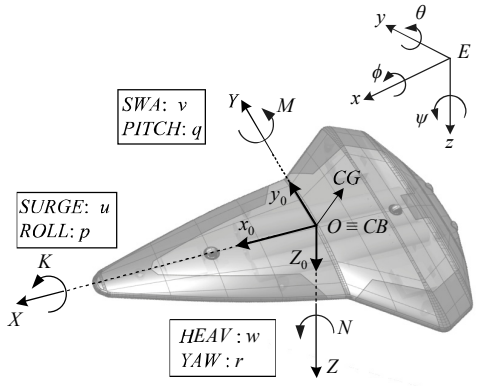

Fig. 3. Coordination systems: $Ox_0y_0z_0$ and $Exyz$ are body-fixed and earth-fixed frame respectively

where, u, v, and w are the linear velocities of the origin O of the body-fixed frame; p, q, and r are the angular velocities in the body-fixed frame; ϕ, θ, and ψ are Euler angles in the earth-fixed frame; x_g, y_g, and z_g are the position of the center of gravity (CG; Figure 3) in the moving frame $Ox_0y_0z_0$; X, Y, and Z are the forces acting on the vehicle in

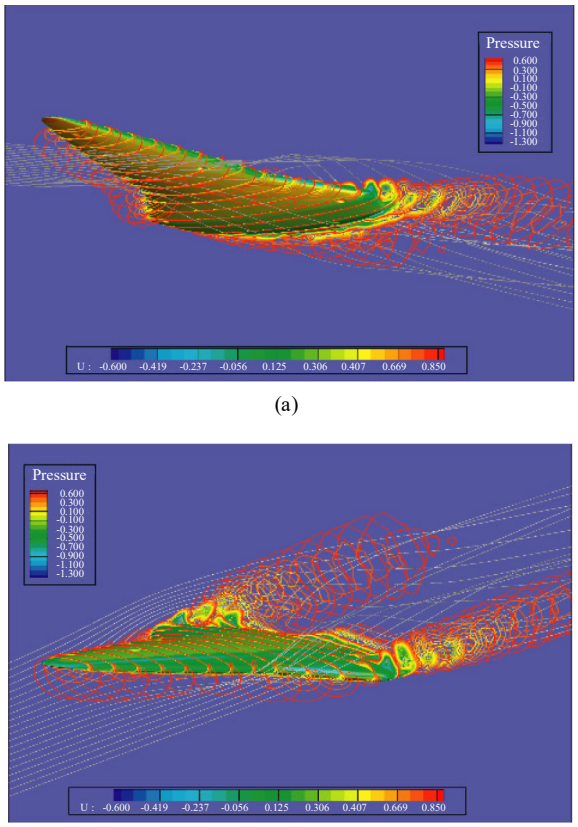

(a)

(b)

Fig. 4. Pressure distribution of RHUG. (a) ascending motion and (b) descending motion

the body-fixed frame; and K, M, and N are the moments acting on the vehicle in the body-fixed frame.

The kinematic system can be written as:

$$\begin{aligned}
\dot{x} &= uc(\psi)c(\theta)+v\big(c(\psi)s(\theta)s(\phi)-s(\psi)c(\phi)\big)\\
&\quad +w\big(s(\psi)s(\phi)+c(\psi)c(\phi)s(\theta)\big)\\
\dot{y} &= us(\psi)c(\theta)+v\big(c(\psi)c(\phi)-s(\phi)s(\theta)s(\psi)\big)\\
&\quad +w\big(s(\theta)s(\psi)c(\phi)-c(\psi)s(\phi)\big)\\
\dot{z} &= -us(\theta)+vc(\theta)s(\phi)+wc(\theta)c(\phi)\\
\dot{\phi} &= p+qs(\phi)t(\theta)+rc(\phi)t(\theta)\\
\dot{\theta} &= qc(\phi)-rs(\phi)\\
\dot{\psi} &= q\frac{s(\phi)}{c(\theta)}+r\frac{c(\phi)}{c(\theta)}
\end{aligned} \tag{2}$$

Here, once $j\in\{\phi;\theta;\psi\}$, then $c(j)$ is $cos(j)$; $s(j)$ is $sin(j)$; and $t(j)$ is $tan(j)$.

3. Dynamics of vertical-plane motion

To simplify the complex 6-DOF model in the previous section, it can be divided to the vertical-plane motion (surge-heave-pitch) and heading motion based on a CFD (computational fluid dynamics) results as shown in Figure 4 and Table 2. The roll and sway dynamics can be neglected when the gliding motion is the target dynamic.

According to the hydrodynamics coefficients, the vertical-plane motion can be expressed as:

$$\begin{aligned}
&\dot{x} = ucos\theta+wsin\theta\\
&\dot{z} = -usin\theta+wcos\theta\\
&\dot{\theta} = q\\
&\big(m-X_{\dot{u}}\big)\dot{u} = -mz_g\dot{q}+mx_gq^2-mwq+Z_{\dot{w}}wq\\
&\qquad +X_{uu}u^2+X_{qq}q^2+X_{ww}w^2+X_{wq}wq\\
&\qquad -\big(W-B\big)sin\theta+\tau_w sin\theta+\tau_u+\tau_{eu}\\
&\big(m-Z_{\dot{w}}\big)\dot{w} = \big(mx_g+Z_{\dot{q}}\big)\dot{q}+mz_gq^2+muq-X_uuq\\
&\qquad +Z_{uu}u^2+Z_qq+Z_ww+Z_{w|w|}w|w|\\
&\qquad +\big(W-B\big)cos\theta+\tau_w cos\theta+\tau_{ew}\\
&\big(I_{yy}-M_{\dot{q}}\big)\dot{q} = -mz_g\dot{u}+\big(mx_g-M_{\dot{w}}\big)\dot{w}-mz_gqw\\
&\qquad -Z_{\dot{w}}wu-Z_{\dot{q}}qu+X_{\dot{u}}uw+M_{uu}u^2+M_qq\\
&\qquad +M_{q|q|}q|q|+M_ww+M_{w|w|}w|w|\\
&\qquad -\big(z_gW-z_bB\big)sin\theta-\big(x_g-x_bB\big)cos\theta+\tau_q+\tau_{eq}
\end{aligned} \tag{3}$$

where, W is the vehicle weight; B is the buoyancy force in the neutral buoyant condition; x_b and z_b are the coordinates of the center of buoyancy; τ_u, τ_w and τ_q are the control inputs induced by the thrusters, buoyancy engines, and moving mass, respectively; τ_{eu}, τ_{ew}, and τ_{eq} are the environmental disturbances in the surge, heave, and pitch motions, respectively. It is noted that τ_w=W-B is the net buoyancy force. When the piston compresses the air inside the buoyancy engine, τ_w will be positive, otherwise, τ_w will be negative. It means that the magnitude of τ_w can be controlled by the position of the piston of the buoyancy engine. The pitch angle of the RHUG is controlled by τ_q which is the moment caused by the change of the center of gravity. And in the RHUG, the center of gravity is adjusted by the position of the 1.5 kg moving mass. In Figure 1, two thrusters in the rear of the RHUG is for heading control.

4. Dual-buoyancy engine experiment

Due to the new hull design of RHUG, the dynamics of RHUG should be verified before other further investigation. Therefore, the gliding motion is conducted in the water tank with descending motion. And the comparison of simulation and experiment is carried out.

The harness assembly of RHUG is constructed as shown in Figure 5. The dual buoyancy is denoted as the left and right buoyancy engines using two BLDC motors due to its high

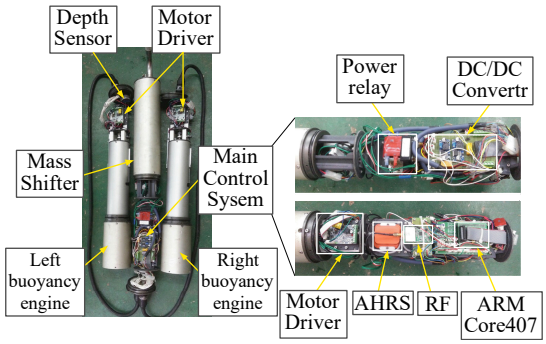

Fig. 5. Hardware structure of RHUG

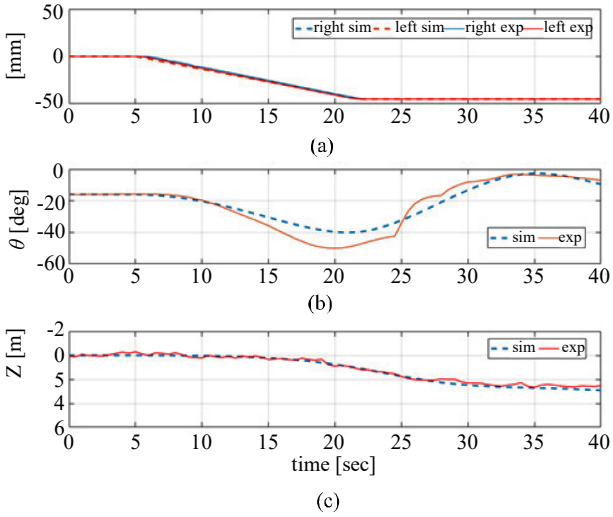

Fig. 6. Simulation and experiment results of descending motion. (a) control inputs of dual buoyancy engine, (b) pitch angle and (c) depth.

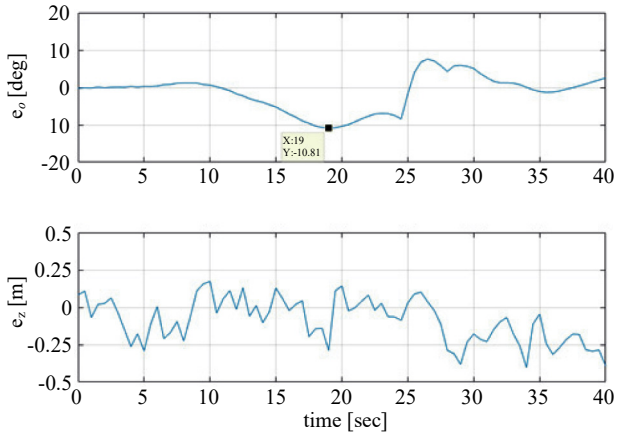

Fig. 7. Modeling error in the descending motion: (a) pitch angle and (b) depth difference between simulation and experiment, respectively.

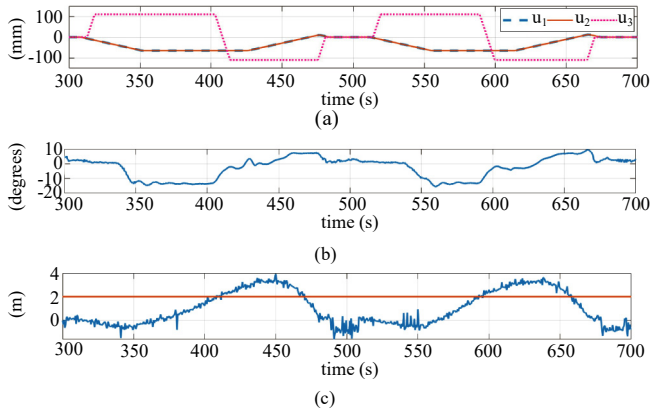

Fig. 8. Diving performance of RHUG in a sea trial.

efficiency. The moving mass is controlled by the mass-shifter using a DC motor. The pitch angle of RHUG is measured by AHRS sensor.

The buoyancy engine is tested in the water tank with constant τ_q. At first, the moving mass is kept at the position so that the pitch angle of the vehicle is negative. Then, the buoyancy engine start to pull back the piston on the left and right in Figure 5. The volume of the vehicle will decrease and when τ_w is positive, the vehicle will move downward. And if the pitch angle is also negative, then it will move forward. For more details, Figure 6 will show the simulation and experiment result for the dual buoyancy engine as followings.

The pitch angle of RHUG is controlled by the moving mass at around −16° as shown in Figure 6b. After 5 seconds, the dual buoyancy engine start to compress the air inside the cylinder. The piston is controlled from 0 mm to -45 mm as shown in Figure 6a. When the buoyancy force is less than the weight of RHUG, the vehicle move down slowly as shown in Figure 6c.

The solid red line is the experiment results, and the dash blue line is the simulation with the developed hydrodynamics coefficients. Figure 6 showed that the tendency of the simulation and experiment results of pitch angle and depth are similar, and then dynamics model of vertical-plane motion is verified. The gap between the simulation and experiment results is shown in Figure 7. The biggest difference in pitch angle is around 10° in Figure 7a. The depth difference is under 0.5m as shown in Figure 7b.

III. SEA TRIAL

Once the descending motion of the new hull design is conducted in the water tank, the gliding motion is next examined by many sea trials. And one of them is presented here in Figure 8. In this sea trial, the pitch angle is fully controlled by the moving mass from -10° to 10° for descending and ascending motion, respectively. In the beginning, the desired pitch angle is set as -10° for the descending movement. And at the same time, the left and right pistons move backward to -60 mm to make the vehicle go down. When the RHUG reaches 2 m (switching depth) in the depth, the pitch angle is controlled to 10° for the ascending motion. But the pistons

are still at −60 mm to prevent the backward motion due to the transient response in the pitch control. Only when the pitch angle is positive, the pistons are allowed to move forward to 60 mm to make the RHUG ascend to the water surface. And then, when the vehicle's depth is less than 0.5 m, both the pistons and the moving mass are commanded to move to 0 mm position. This operation is one cycle of the gliding motion.

The control input of the dual buoyancy engine and the mass-shifter are presented in Figure 8a. The pink dotted line presents the moving mass position inside the mass-shifter. The dash blue and solid red lines represent left and right piston position, respectively. The pitch angle and depth are shown in Figure 8b-c. The switching depth between descending and ascending motion is set at 2m as the solid red line in Figure 8c.

At the beginning, the vehicle is in zero pitch angle. When the moving mass moves forward, the pitch angle decrease to negative value as shown in Figure 8b. At the same time, the dual buoyancy engine compresses the air inside the hull and create negative net buoyancy force which exerts the vehicle to glide down as shown in Figure 8c.

If the vehicle depth is greater than 2m (red solid line in Figure 8c), the moving mass goes backward to pitch the vehicle up before ascending. The net buoyancy engine is kept compressed until the pitch angle is greater than -5°. The ascending motion of the vehicle is performed when the buoyancy engine enlarge its volume with an enough amount of net buoyancy force. And repeating this process will perform another gliding motion. Two cycles of diving are conducted and showed in Figure 8b-c.

IV. CONCLUSIONS

A RHUG dynamics was developed for vertical-plane motion using the CFD results of the ray-type hull. The hydrodynamics coefficients were presented for the gliding motion. This model was verified through the experiment of descending motion in the water tank. A comparison between simulation and experiment was carried out with a same tendency. The sea experiment of RHUG was performed to validate the new hull design. The experiment showed a good gliding motion using moving mass and dual-buoyancy engine. Therefore, this investigation will open a new way to develop long-range underwater glider with large buoyancy capacity.

ACKNOWLEDGMENTS

This is results of the research project entitled "data collecton system with underwater glider" (19-SN-MU-01) and is a part of the result of the research project (18-SN-RB-01).

REFERENCES

Cao, J., D. Lu,, D. Li,, Z. Zeng,, B. Yao, and L. Lian, (2019). Smartfloat: A Multimodal Underwater Vehicle Combining Float and Glider Capabilities. IEEE Access, 7, 77825-77838.

Ma, Y., G. Pan,, Q. Huang, and Y. Shi (2018). Research on fluid dynamic layout of blend wing body underwater glider with tail. In 2018 OCEANS-MTS/IEEE Kobe Techno-Oceans (OTO) (pp. 1-6). IEEE.

Nakamura, M., K. Asakawa, T. Hyakudome, S. Kishima, H. Matsuoka and T. Minami (2013). Hydrodynamic coefficients and motion simulations of underwater glider for virtual mooring. IEEE Journal of Oceanic Engineering 38(3), 581-597.

Sherman, J., R. E. Davis, W. B. Owens and J. Valdes (2001). The autonomous underwater glider" Spray". IEEE Journal of Oceanic Engineering 26(4), 437-446.

Smith, R. N. and V. T. Huynh (2013). Controlling buoyancy-driven profiling floats for applications in ocean observation. IEEE Journal of Oceanic Engineering 39(3), 571-586.

Wang, Z., Y. Li, A. Wang and X. Wang (2015). Flying wing underwater glider: Design, analysis, and performance prediction. In 2015 International Conference on Control, Automation and Robotics, 74-77.

Webb, D. C., P. J. Simonetti and C. P. Jones (2001). SLOCUM: An underwater glider propelled by environmental energy. IEEE Journal of Oceanic Engineering 26(4), 447-452.

Zhang, F., J. Thon, C. Thon and X. Tan (2013). Miniature underwater glider: Design and experimental results. IEEE/ASME Transactions on Mechatronics 19(1), 394-399.